Reaction Front Propagation in Nonadiabatic Exothermic Reaction Flow Systems

A general analysis of the reaction wave propagation in nonlinear exothermic nonadiabatic diffusion-convection-reaction systems is presented. The following topics are considered: approximation of temperature profiles based on the idea of infinitesimaly thin reaction front, estimation of maximum temperature, estimation of the conversion at the hot spot, *a priori* calculation of the front velocity, analysis of the self-ignition phenomena and their relation to wave propagation, and discussion of the effect of the heat loss parameter on the direction of propagation and shape of traveling waves. A comparison of the analytical work with exact numerical results reveals excellent agreement. The main objective of this paper is to provide a definite analysis of reaction wave propagation in reacting flow systems.

J. E. Gatica, Jan Puszynski
Vladimir Hlavacek
Department of Chemical Engineering
State University of New York at Buffalo
Amherst, NY 14260

Introduction

The occurrence of exothermic reactions in heterogeneous reacting flow systems is accompanied by a complicated interaction of flow, heat conduction, and mass diffusion. In such systems strongly exothermic reactions may give rise to reaction fronts. The propagation of reaction fronts plays an important role in many chemically reacting systems as, for example, tubular catalytic and noncatalytic reactors, combustion, and flame propagation, so that its detailed description and understanding seem to be desirable.

A theory of propagation of reaction fronts in exothermic systems was initiated by Zel'dovich and Frank-Kamenetskii (1938). Later, Hirschfelder et al. (1953) attempted to develop procedures toward solving the set of coupled nonlinear ordinary differential equations that describe propagation of a laminar flame. Although the problem proved to be too difficult to solve by the methods that they employed, some quantitative results were obtained. In the 1960's and 1970's propagation of reaction fronts in exothermic reacting systems became an important problem for the chemical engineering community, and contributions from Amundson, Wicke, and Vortmeyer and their coworkers in the following papers represent new developments in the field: Liu and Amundson (1962), Rhee et al. (1973), Rhee and Amundson (1974), Padberg and Wicke (1967), Fieguth and Wicke (1971), Vortmeyer and Jahnel (1972), Simon and Vortmeyer (1977), and Kalthoff and Vortmeyer (1980).

The use of activation-energy asymptotics, early initiated in the 1940's by the Russian school and later developed systematically by Western combustion scientists, provides a route to deal with the highly nonlinear reaction term. By using methods of asymptotic analysis, the description of reaction systems has been greatly simplified and new results on reaction front propagation phenomena have been derived. Thus, among other authors, Buckmaster and Ludford (1983), Matkowsky and Sivashinsky (1979), Matkowsky and Olagunju (1981), Sivashinsky and Matkowsky (1981), Margolis (1983, 1985), and Margolis and Armstrong (1985) have presented important results on propagation of reaction fronts in adiabatic and nonadiabatic homogeneous exothermic reaction systems.

The present paper makes an attempt to analyze globally wave propagation phenomena in nonadiabatic exothermic reaction flow systems. The analysis is based on the old idea by Zel'dovich and Frank-Kamenetskii (1938) and Frank-Kamenetskii (1969) which assumes that the reaction occurs only inside a narrow zone and outside this zone only heat and mass transfer phenomena take place.

The contribution of this paper is an analytical and numerical study of propagation phenomena in exothermic nonadiabatic systems. *A priori* direct formulas that can be applied to both downstream and upstream propagating waves, were developed for the velocity of the reaction front, for the temperature and conversion at the hot spot and for the ignition length. The results of this analysis are in satisfactory agreement with exact results furnished by numerical integration of the full governing equations.

The present paper also describes the application of the analy-

Correspondence concerning this paper should be addressed to Vladimir Hlavacek.

sis to reacting systems where multiplicity phenomena occur. The developed analytical tools make it possible to make a good *a priori* estimates about:

1. The shape of the propagating profiles (constant pattern profiles or degenerated waves)
2. The direction and speed of propagation
3. Self-ignition development

Description of the Reacting System

This paper concerns the propagation of reaction fronts through a gaseous flow system. The problem is: What kind of wave, traveling or standing, can we expect for given system parameters and initial conditions? What is the direction of the wave and how to calculate *a priori* the speed of the wave? The analysis presented below provides an escape from the intractability of the nonlinear governing equations; it will be shown that the flame sheet approximation provides all necessary tools to develop a complete analysis.

The analysis presented here can be applied directly to packed catalytic reactors, laminar flames, and filtration combustion problems (combustion of gas in solid noncatalytic packing). Many features of the analysis can be utilized even for noncatalytic gas-solid exothermic problems.

To make the problem tractable we decouple the fluid flow equations from the heat and mass transfer equations. This strategy was first used by Zel'dovich et al. (1938, 1980) and Frank-Kamenetskii (1969) in their famous attempt to develop a description of laminar flame propagation in gaseous systems. The resulting set of equations is called in the combustion oriented literature "the diffusion model of a laminar flame." The idea of decoupling was systematically used by chemical engineers in the design of nonadiabatic reactors, and description of parametric sensitivity and wave propagation in nonisothermal reacting systems. The qualitative and quantitative aspects of this approximation can be found elsewhere (Clavin, 1985; Zel'dovich et al., 1980).

For the mathematical description of the heat and mass transfer processes in fixed-bed reactors, two general types of models have been developed:

1. The one-phase, or pseudohomogeneous model, in which the reactor is approximated by a quasi-continuum medium
2. The two-phase model, in which mass and heat transfer processes are considered in both solid and fluid phases

The following analysis is relevant to a one-phase model. The governing transport equations describing heat and mass transfer in a reacting convective system, which is decoupled from the flow equations, are:

$$\epsilon \frac{\partial y}{\partial t} = -\epsilon u \frac{\partial y}{\partial z} + D_{ez} \frac{\partial^2 y}{\partial z^2} + \frac{1}{C_o} R(y, T) \tag{1}$$

$$\rho_g C_{pg} \epsilon \sigma \frac{\partial T}{\partial t} = -\rho_g C_{pg} \epsilon u \frac{\partial T}{\partial z} + k_{ez} \frac{\partial^2 T}{\partial z^2} + (-\Delta H_r) R(y, T) - \frac{4U}{D_t}(T - T_o) \tag{2}$$

where

$$R(y, T) = k_o \exp\left(-\frac{E}{RT}\right) f(y)$$

and

$$\sigma = \frac{[\rho_g C_{pg} \epsilon + \rho_s C_{ps}(1 - \epsilon)]}{\rho_g C_{pg} \epsilon}$$

or, in a dimensionless form

$$\frac{\partial y}{\partial \tau} = -\frac{\partial y}{\partial \eta} + \frac{1}{Bo_z} \frac{\partial^2 y}{\partial \eta^2} + Da \exp\left(\frac{\theta}{1 + \frac{\theta}{\gamma}}\right) f(y) \tag{3}$$

$$\sigma \frac{\partial \theta}{\partial \tau} = -\frac{\partial \theta}{\partial \eta} + \frac{1}{Pe_z} \frac{\partial^2 \theta}{\partial \eta^2} + BDa \exp\left(\frac{\theta}{1 + \frac{\theta}{\gamma}}\right) f(y) - \beta\theta \tag{4}$$

subject to the following boundary conditions

$$\frac{\partial y}{\partial \eta} = Bo_z y \quad \frac{\partial \theta}{\partial \eta} = Pe_z \theta \quad \text{at } \eta = 0 \tag{5}$$

and

$$\frac{\partial y}{\partial \eta} = \frac{\partial \theta}{\partial \eta} = 0 \quad \text{at } \eta = 1 \tag{6}$$

In our discussion of propagation of reaction fronts in nonlinear exothermic reaction systems, the breaking of symmetry phenomena will be neglected. The crucial assumption made is a planar stable reaction front. The radial distribution of temperature resulting from the lateral cooling of the system is also neglected. In many nonadiabatic nonisothermal systems the integral, radially averaged temperature represents a satisfactory approximation (Hlavacek and Votruba, 1977). As a result, the one-dimensional situation alone will be addressed.

The relevant assumptions used to develop approximate analytical formulas are summarized below:

1. A strongly exothermic, irreversible reaction with high activation energy is carried out. A narrow reaction zone located close to the maximum temperature is assumed.
2. The velocity field is decoupled from the governing heat and mass balances.
3. A stable planar reaction front is considered.
4. The reaction rate is negligible in the preheating and quenching zones; see Figure 1.
5. The axial mass diffusion effects are negligible.
6. The reaction front is located far from the reactor inlet and outlet and can propagate with constant velocity w.
7. All physical properties are considered constant and evaluated at inlet conditions. The temperature of the surroundings is assumed constant.

If the temperature and conversion profiles (and consequently, the reaction front) propagate with constant speed w and without changing their shape (constant pattern profiles), a similarity transformation (Frank-Kamenetskii, 1969; Rhee et al., 1974) can be used to simplify the governing transient equations $x = z - wt$ and $\tau = t$, and the governing Eqs. 1 and 2 can be written as follows

$$\epsilon(u - w) \frac{dy}{dx} = \frac{1}{C_o} R(y, T) \tag{7}$$

Table 1. Values of Variables and Parameters

T_o, K	Y_o	Da	B
243	0.02	0.4034	11.8737
	0.03	0.4034	17.8106
263	0.03	1.1261	15.5063
	0.035	1.1261	18.0906
293	0.03	4.3185	12.8368

$G_m = (\rho_g u)_o = 9.26\ 10^{-2}$ kg · m^{-2} · s^{-1}
$L = 0.060$ m; $D_t = 0.023$ m; $D_p = 0.0034$ m
$Bo_z = 465.88$*; $Pe_z = 38.84$*; $\sigma = 2{,}139.73$

Rate Expression

$$R(y,T) = k_o \exp\left(-\frac{E}{RT}\right)\left[\frac{C_o(1-y)}{1 + K_{eq}\, C_o(1-y)}\right]$$

where

$k_o = 7.42\ 10^6$ s^{-1}
$E/R = 6{,}396.9$ K
$K_{eq} = 2{,}959.39$ m$_g^3$ · kmol$_{CO}^{-1}$

*Values of axial mass and thermal Peclet numbers calculated from correlations proposed by Edwards and Richardson (1968) and Votruba et al. (1972), respectively.

$$\rho_g C_{pg}\epsilon(u - \sigma w)\frac{dT}{dx} = k_{ez}\frac{d^2T}{dx^2} + (-\Delta H_r)R(y,T) - \frac{4U}{D_t}(T - T_o) \quad (8)$$

The values of the parameters for the calculations as well as the rate expression, reported in Table 1, have been chosen for a catalytic packed bed where the oxidation of carbon monoxide over Pt/Al_2O_3 is carried out (Puszynski and Hlavacek, 1980).

Approximation of temperature profiles

Outside the reaction zone, Figure 1, the heat balance, Eq. 8, has the form

$$k_{ez}\frac{d^2T}{dx^2} + \rho_g C_{pg}\epsilon(\sigma w - u)\frac{dT}{dx} - \frac{4U}{D_t}(T - T_o) = 0 \quad (9)$$

To remove the end effects, an infinitely long system will be considered. The boundary conditions will assume the form:

Preheating zone

$$T = T_o \quad \text{and} \quad \frac{dT}{dx} = 0 \quad \text{for } x \to -\infty \quad (10)$$

Quenching zone

$$T = T_o \quad \text{and} \quad \frac{dT}{dx} = 0 \quad \text{for } x \to +\infty \quad (11)$$

Since the reaction is strongly exothermic and $E/RT_m \gg 1$, we can assume that the reaction zone thickness is negligible compared to the preheating and quenching zone lengths. As a result, the following matching condition can be imposed

$$\lim_{x\to 0^+} T = \lim_{x\to 0^-} T = T_m \quad (12)$$

The eigenvalues of the solution to Eq. 9 are

$$\lambda_{1,2} = \frac{1}{2}\frac{\rho_g C_{pg}\epsilon(u - \sigma w)}{k_{ez}} \cdot \left[1 \pm \sqrt{1 + \frac{16Uk_{ez}}{D_t\rho_g^2 C_{pg}^2\epsilon^2(u - \sigma w)^2}}\right] \quad (13)$$

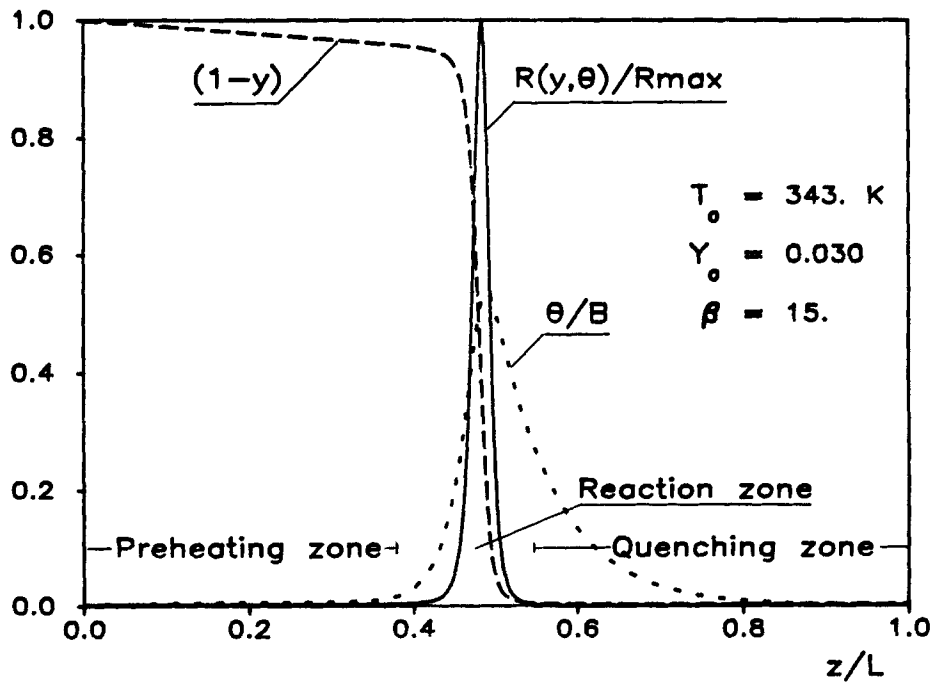

Figure 1. Zones identifiable in a reacting flow system.

In order to satisfy the boundary conditions, Eqs. 10 and 11, the solution in each zone must be represented by just one eigenvalue. Thus, the solution to Eq. 9 reads

$$(T - T_o)_{1,2} = (T_m - T_o) \exp(\lambda_{1,2} x) \tag{14}$$

where 1 and 2 stand for preheating and quenching zone, respectively, and the inequality in Eq. 15 holds for eigenvalues λ_1 and λ_2

$$\lambda_2 \leq 0 < \lambda_1 \tag{15}$$

To satisfy the above inequality, the following restriction for the front velocity has to be satisfied

$$w < \frac{u}{\sigma} \tag{16}$$

Estimation of maximum temperature

Equations 7 and 8 can be combined to eliminate the reaction term. The resulting equation reads

$$k_{ez}\frac{d^2T}{dx^2} - \rho_g C_{pg}\epsilon(\sigma w - u)\frac{dT}{dx} - \frac{4U}{D_t}(T - T_o) - (-\Delta H_r)C_o\epsilon(w - u)\frac{dy}{dx} = 0 \tag{17}$$

The above equation can be integrated across the reaction zone, Figure 2, subject to

$$y = 0, \quad T = T\Big|_{-\Delta\xi/2}, \quad \text{and} \quad \frac{dT}{dx} = \frac{dT}{dx}\Big|_{-\Delta\xi/2} \quad \text{at } x = -\frac{\Delta\xi}{2}$$

and

$$y = 1, \quad T = T\Big|_{+\Delta\xi/2}, \quad \text{and} \quad \frac{dT}{dx} = \frac{dT}{dx}\Big|_{+\Delta\xi/2} \quad \text{at } x = +\frac{\Delta\xi}{2}$$

and the following expression results

$$k_{ez}\left[\frac{dT}{dx}\Big|_{\Delta\xi/2} - \frac{dT}{dx}\Big|_{-\Delta\xi/2}\right] - \rho_g C_{pg}\epsilon(\sigma w - u)(T|_{+\Delta\xi/2} - T|_{-\Delta\xi/2}) - \frac{4U}{D_t}\int_{-\Delta\xi/2}^{\Delta\xi/2}(T - T_o)dx - (-\Delta H_r)C_o\epsilon(w - u) = 0 \tag{18}$$

For an infinitesimally narrow reaction zone ($\Delta\xi \to 0$) the second and third terms in Eq. 18 become negligible compared with the conductive term, and the following relation between heat fluxes results

$$k_{ez}\left[\frac{dT}{dx}\Big|_{0+} - \frac{dT}{dx}\Big|_{0-}\right] \simeq \rho_g C_{pg}\epsilon(w - u)(T_a - T_o) \tag{19}$$

The temperature gradients in Eq. 19 can be evaluated from the expression for the temperature profiles derived in the previous section, Eq. 14.

The final expression, which relates hot spot temperature, propagation velocity of the reaction front, and system parameters, is

$$\left(\frac{T_a - T_o}{T_m - T_o}\right)\left(\frac{u - w}{u - \sigma w}\right) = \sqrt{1 + \frac{16Uk_{ez}}{D_t\rho_g^2 C_{pg}^2\epsilon^2(u - \sigma w)^2}}$$

or, in dimensionless form

$$\frac{B}{\theta_m}\left(\frac{1 - w}{1 - \sigma w}\right) = \sqrt{1 + \frac{4\beta}{Pe_z(1 - \sigma\omega)^2}} \tag{20}$$

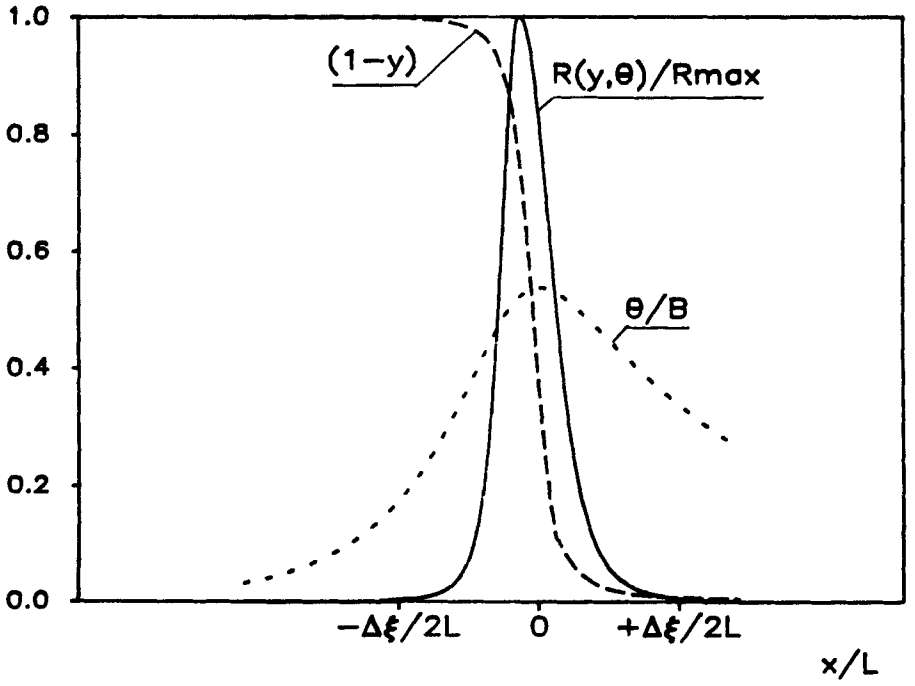

Figure 2. Model of reaction zone.

The above relation indicates that the maximum temperature in the reactor can exceed the adiabatic temperature only for a downstream propagating wave ($\omega > 0$).

In the adiabatic reactor ($\beta = 0$), the maximum temperature (θ_m) is equal to the adiabatic temperature B only if the steady state is reached ($\omega = 0$).

Estimation of conversion at the hot spot

The value of the conversion y_m, Figure 2, can be estimated by integration of Eq. 17 subject to

$$y = 0, \quad T = T_o, \quad \text{and} \quad \frac{dT}{dx} = 0 \quad \text{for } x \to -\infty$$

and

$$y = y_m, \quad T = T_m, \quad \text{and} \quad \frac{dT}{dx} = 0 \quad \text{for } x = 0$$

The resulting equation has the form

$$\rho_g C_{pg}\epsilon(\sigma w - u)(T_m - T_o) - \frac{4U}{D_t}\int_{-\infty}^{0}(T - T_o)\,dx - (-\Delta H_r)C_o\epsilon(w - u)y_m = 0$$

This equation can be rearranged to:

$$y_m = \left(\frac{u - \sigma w}{u - w}\right)\left(\frac{T_m - T_o}{T_a - T_o}\right) + \frac{4U}{D_t\rho_g C_{pg}\epsilon(T_a - T_o)(u - w)}\int_{-\infty}^{0}(T - T_o)\,dx \quad (21)$$

After neglecting the thickness of the reaction zone and using Eq. 14, the integral in the above equation can be approximated by

$$\int_{-\infty}^{0}(T - T_o)\,dx \simeq \frac{T_m - T_o}{\lambda_1}$$

Here λ_1 is given by Eq. 13.

By using this approximation a relation between the front properties and system parameters can be obtained

$$y_m = \frac{1}{2}\left(\frac{T_m - T_o}{T_a - T_o}\right)\left(\frac{u - \sigma w}{u - w}\right)\left[1 + \sqrt{1 + \frac{16\,Uk_{ez}}{D_t\rho_g^2 C_{pg}^2\epsilon^2(u - \sigma w)^2}}\right]$$

or, in dimensionless form

$$y_m = \frac{1}{2}\frac{\theta_m}{B}\left(\frac{1 - \sigma\omega}{1 - \omega}\right)\left[1 + \sqrt{1 + \frac{4\beta}{Pe_z(1 - \sigma\omega)^2}}\right] \quad (22)$$

Estimation of front velocity

To describe the temperature and conversion profiles inside the reaction zone, Eq. 17 can be integrated subject to

$$y = y_m, \quad T = T_m, \quad \text{and} \quad \frac{dT}{dx} = 0 \quad \text{at } x = 0$$

and

$$y = y, \quad T = T, \quad \text{and} \quad \frac{dT}{dx} = \frac{dT}{dx} \quad \text{for } x\epsilon\left(-\frac{\Delta\xi}{2}, \frac{\Delta\xi}{2}\right)$$

The resulting equation has the form

$$k_{ez}\frac{dT}{dx} + \rho_g C_{pg}\epsilon(\sigma w - u)(T_m - T) - \frac{4U}{D_t}\int_x^0 (T - T_o)\,dx - (-\Delta H_r)C_o\epsilon(w - u)(y_m - y) = 0 \quad (23)$$

It has been indicated above that the terms accounting for the convective transport and heat losses inside the narrow reaction zone are negligible compared to the conductive transport. Based on this assumption, Eq. 23 becomes

$$k_{ez}\frac{dT}{dx} = (-\Delta H_r)C_o\epsilon(u - w)(y_m - y) \quad (24)$$

This equation can be combined with the mass balance, Eq. 7, to eliminate the independent variable x:

$$k_{ez}\frac{dT}{dy} = (-\Delta H_r)C_o^2\epsilon^2(u - w)^2\left(\frac{y_m - y}{R(y, T)}\right) \quad (25)$$

The resulting Eq. 25 can be integrated subject to the boundary conditions, Figure 2, $T = T_m$ at $y = y_m$, and $T = T|_{-\Delta\xi/2}$ at $y = 0$, giving:

$$(u - w)^2 = \frac{k_o k_{ez}}{(-\Delta H_r)C_o^2\epsilon^2}\left(\frac{RT_m^2}{E}\right)\left[\frac{\exp\left(-\frac{E}{RT_m}\right)}{F(y_m)}\right]$$

or, in dimensionless form

$$(1 - \omega)^2 = \frac{Da}{Pe_z B}\left(\frac{\theta_m}{B} + 1\right)^2 \exp\left(\frac{\theta_m}{1 + \frac{\theta_m}{\gamma}}\right)\left[\frac{1}{C_o F(y_m)}\right] \quad (25)$$

Here $F(y_m) = \int_0^{y_m}[(y_m - y)/f(y)]\,dy$.

The above expression, Eq. 25, was obtained by using the assumption that for a strongly exothermic reaction with high activation energy, the following approximation (Zel'dovich et al., 1980) can be applied

$$\int_{T|_{-\Delta\xi/2}}^{T_m}\exp\left(-\frac{E}{RT}\right)dT \simeq \frac{RT_m^2}{E}\exp\left(-\frac{E}{RT_m}\right)$$

Ignition and Wave Propagation

In the previous section the formulas to estimate the properties of propagating fronts in nonadiabatic exothermic reacting flow systems have been developed. These expressions are based on the assumption of a reaction front located far enough from the reactor inlet or outlet, and unicity of steady state solutions. However, these assumptions are not always satisfied.

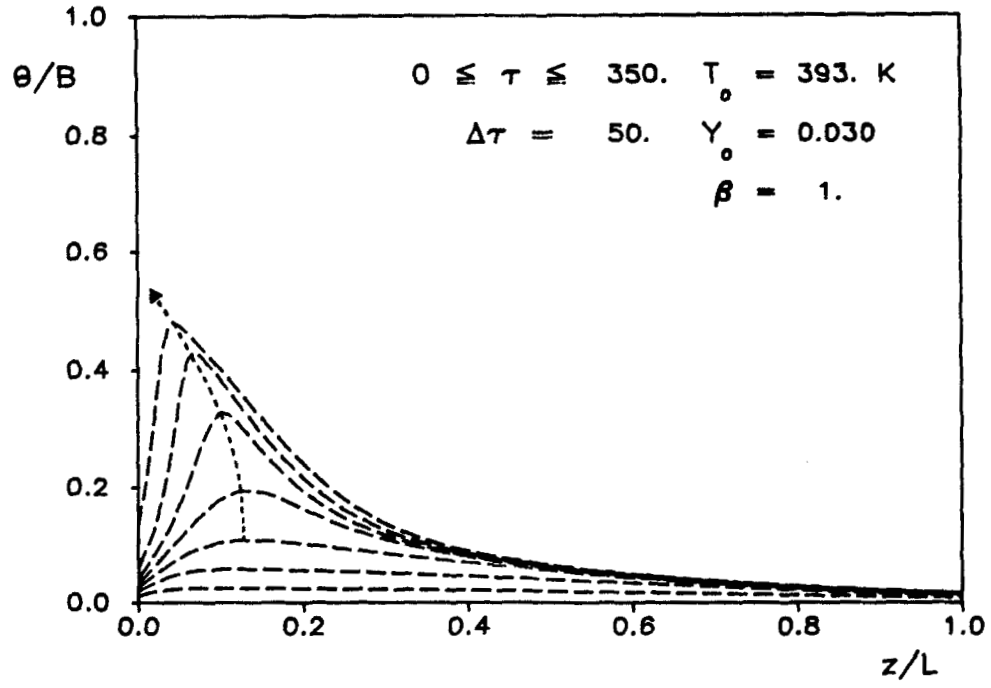

Figure 3. Ignition as a degenerated wave.

For a reactor of a finite length, the following situations can be expected:

1. The catalytic bed is long enough to exhibit a self-ignition process, which results in a formation of a temperature wave. Only one ignited steady state (ISS) is possible. ISS is characterized by steep temperature and conversion profiles.
2. The reactor cannot be self-ignited, but multiple steady states can exist.
3. A self-ignition process does not occur and the reactor can operate only at an extinguished steady state (ESS). ESS is characterized by flat temperature and conversion profiles.

In the case of only one ISS, the reactor can be ignited anywhere (depending on the operating conditions) inside the system. When the reactor is ignited close to the entrance, a propagating wave cannot develop and a degenerated standing wave results, Figure 3. For an ignition process taking place far enough from the entrance, traveling waves will develop, Figure 4, and our approximate formulas can be used.

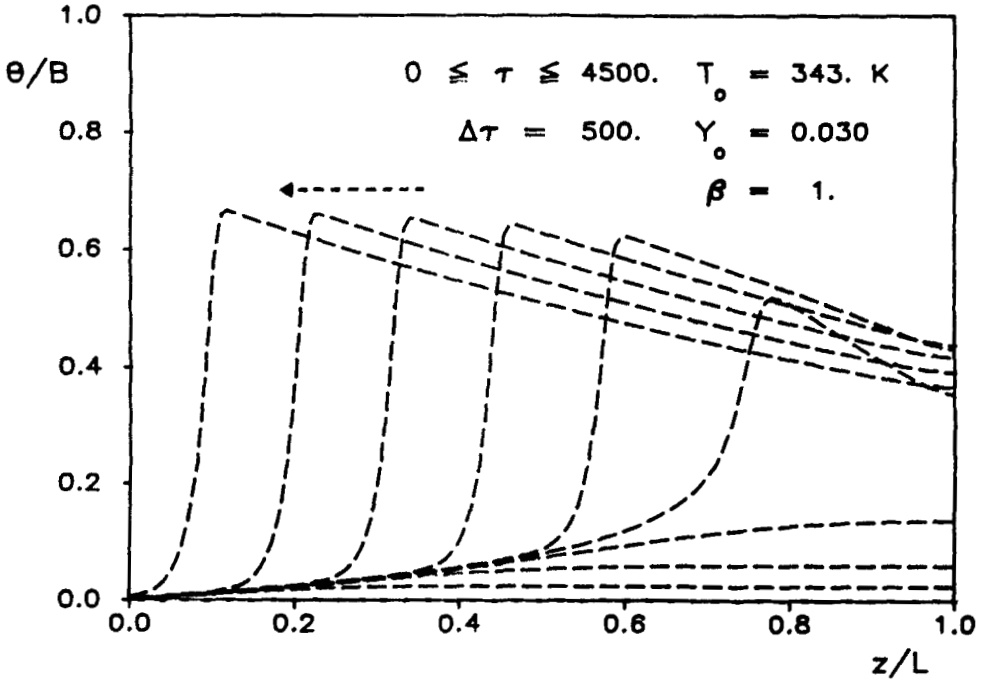

Figure 4. Ignition as a traveling wave.

Let us now define the ignition length, z_i, as the distance from the reactor entrance to the position of the maximum reaction rate at the moment of ignition. It is evident from Figures 3 and 4 that the ignition length is crucial for the analysis of wave propagation in reacting flow systems.

Estimation of ignition length

For preignition conditions low consumption of the reactants can be assumed and the concentration term of the reaction rate expression can be approximated by using the inlet conditions. Thus, for quasi steady state conditions in the preignition regime, the dimensionless energy balance has the form

$$\frac{d\theta}{d\eta} = BDa\left(\frac{f(y)}{C_o}\bigg|_{y=0}\right)\exp\left(\frac{\theta}{1+\frac{\theta}{\gamma}}\right) - \beta\theta \qquad (27)$$

subject to $\theta = 0$ at $\eta = 0$ and $\theta = \theta_i$ at $\eta = \eta_i$.

An approximate analytical expression relating the ignition length, ignition temperature, and system parameters can be obtained if the nonlinear righthand side of Eq. 27 is linearized around $\theta = 0$.

$$\eta_i = \frac{1}{C}\frac{1}{\left(1-\frac{\beta}{C}\right)}\ln\left[1+\theta_i\left(1-\frac{\beta}{C}\right)\right] \qquad (28)$$

where $C = BDa(f(y)/C_o|_{y=0})$

Here, the ignition temperature θ_i is considered as the temperature at which the derivative of the reaction rate with respect to temperature becomes maximum, and it can be estimated from the relation derived by Babkin et al. (1983) as

$$\theta_i = \tfrac{1}{2}\gamma\sqrt{B} - (B+\gamma) \qquad (29)$$

The value of the ignition length can be determined from Eq. 28 after substitution for θ_i from Eq. 29. To obtain exact values of the ignition length, Eq. 27 must be integrated numerically.

Effect of Heat Losses on Wave Propagation

The analysis presented in previous sections allows us to predict analytically the speed and direction of propagation of the reaction front as well as the ignition length. In this section the effect of the heat loss for inlet conditions (inlet temperature, concentration, and gas velocity) that guarantee the developing of a self-ignition process under adiabatic conditions will be analyzed.

The general features of transient behavior of a nonadiabatic reacting flow systems, operating under conditions mentioned above, can be inferred from Figures 12a and 12b. Curve *1* represents the axial position η_i where the ignition process begins. This curve is calculated by numerical integration of Eq. 27 or from Eq. 28. If the value of η_i is in the region $\eta_i \epsilon (0, 1)$, the self-ignition process takes place. If $\eta_i > 1$, then the reactor is too short and self-ignition cannot occur. Curve *2* describes the relation between the reaction front speed and the heat loss parameter as predicted by Eqs. 20, 22, and 25. When the values of the front velocity are negative, the constant pattern profiles will be observed only for upstream propagating waves. On the other hand, when the velocity is positive the constant pattern profiles will be observed only for downstream propagating waves.

When multiple steady states exist the situation becomes more complex and both upstream and downstream waves can be expected. Curve *3* represents the locus of the hot spot position of an unstable steady state η_{US}. This curve was calculated by numerical integration of the governing Eqs. 3 and 4.

When the instant position η_F of a traveling wave (axial location of the hot spot) is in the region between the reactor inlet and the axial position of the unstable steady state (i.e., $0 < \eta_F < \eta_{US}$), the wave will always propagate upstream. Otherwise ($\eta_F > \eta_{US}$),

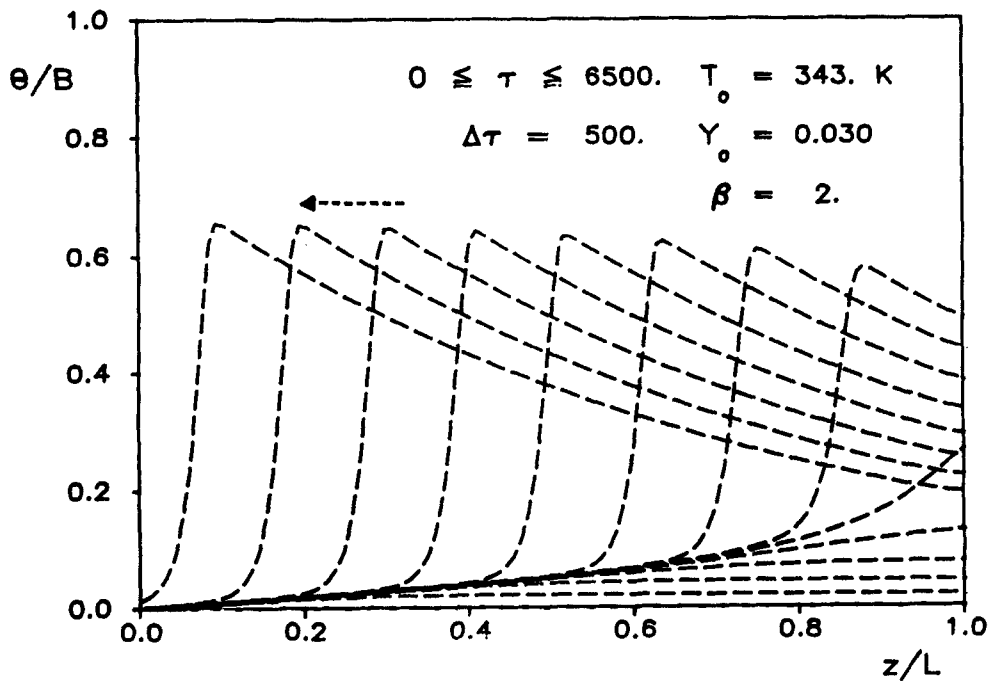

Figure 5. Ignition at the end of the catalytic bed.

the wave will propagate downstream and the ESS steady state will result.

Depending on the values of the heat loss parameter β, different features of the propagating waves can be observed. For values of $\beta < \beta_L$ a self-ignition process occurs in the reactor ($\eta_i < 1$), the reactor front will always propagate upstream, and the ISS steady state will result.

In the region $I(0 < \beta < \beta_L)$ constant pattern profiles can be formed when the ignition process develops far enough from the reactor entrance, Figure 4, and the velocity of the propagating front can be predicted from curve *2*. In turn, when the ignition process takes place close to the reactor entrance ($\eta_i \rightarrow 0$) a "standing-like" wave results, Figure 3, and our analytical formulas cannot be applied.

For $\beta = \beta_L$ an ignition process begins exactly at the end of the reactor, Figure 5. For values of $\beta > \beta_L$ the picture becomes more complicated; the self-ignition process does not occur, but multiple steady states can exist. The multiplicity region can exist only for $\beta_L < \beta < \beta_M$; for higher values of the heat loss parameter ($\beta > \beta_M$), the reactor can operate only at the extinguished steady state, ESS, and downstream waves ($\omega > 0$) can be observed.

When the values of the heat loss parameter are in the interval $\beta_L < \beta < \beta_o$, both upstream (for $0 < \eta_F < \eta_{US}$, region IIa) and downstream (for $\eta_{US} < \eta_F < 1$, region IIb) propagating waves can be observed. The upstream waves will propagate as constant pattern profiles with velocity predicted by curve *2*, Figure 6, while the downstream traveling waves are degenerated (the hot spot temperature will decrease with time).

In region III upstream (for $0 < \eta_F < \eta_{US}$, region IIIa) and downstream (for $\eta_{US} < \eta_F < 1$, region IIIb), waves can be observed. Constant pattern profiles can be expected only for downstream propagating waves (region IIIb). The waves propagating upstream are degenerated (the hot spot temperature will increase with time).

For supercritical values of the heat loss parameter β, $\beta > \beta_{cr}$, the set of Eqs. 20, 22, and 25 does not exhibit a solution. As a result, the constant pattern profiles cannot be formed. If $\beta_M < \beta < \beta_{cr}$ (region IVa, Figure 12a), the waves propagating downstream are constant pattern profiles, Figure 7, while for $\beta_{cr} < \beta < \beta_M$ (region IVb, Figure 12b), degenerated waves traveling both downstream and upstream result, Figure 9.

In region V multiple steady states cannot exist, and $\beta > \beta_{cr}$. Evidently only degenerated waves traveling downstream can be formed, Figure 8.

In reacting flow systems with a strong exothermic reaction, wave propagation can be degenerated. Due to the reactant consumption in the preheating zone (nonzero reaction rate), true constant pattern profiles do not exist in such systems. Numerical results (Puszynski et al., 1986) have shown that for low values of the activation energy, the conversion in the preheating zone can differ significantly from zero; for such conditions, only degenerated waves can be observed. If the activation energy is large, the consumption in the preheating zone becomes less significant, and for certain conditions (T_o, C_o, β, u), a wave can propagate like a constant pattern profile. The ideal constant pattern profiles can be expected only when the activation energy becomes infinity. In real systems with strongly exothermic reactions, typical values of the activation energy range from 50 to 150 *kJ/kmol*.

Numerical Integration of the Reacting Flow

The numerical solution of nonlinear reaction-convection-diffusion equations is a difficult task (McDonald, 1979; Oran and Boris, 1981). This subject is even more difficult when the equations assume a hyperbolic character as a result of the domination of the convective term (Hlavacek and Votruba, 1977).

Price et al. (1966) were the first to recognize that for linear

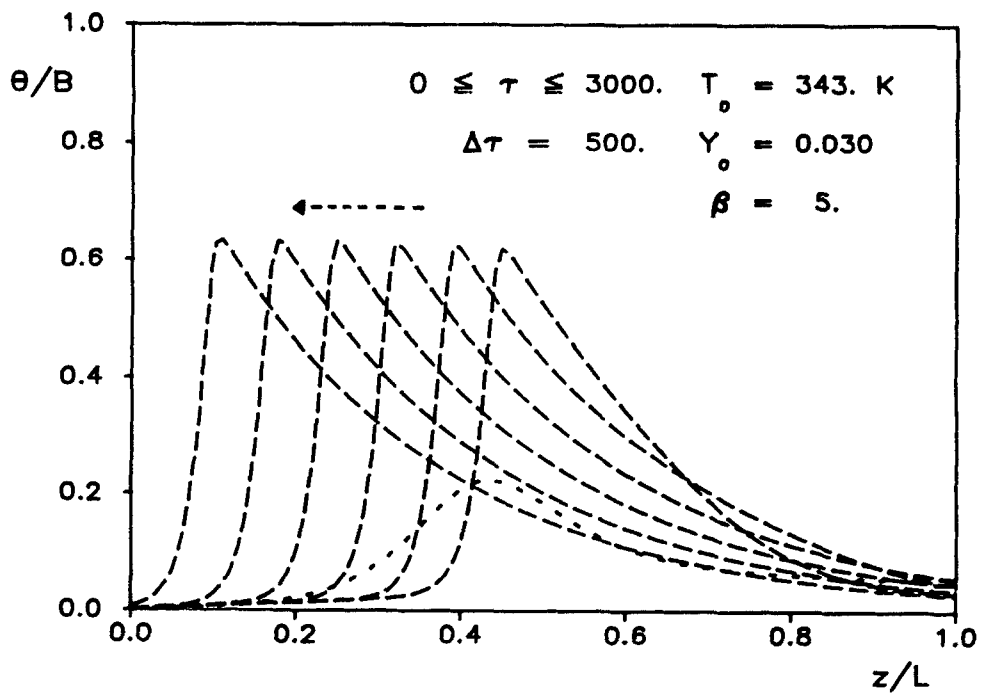

Figure 6. Upstream traveling waves in the region of multiplicity.
Step perturbation in inlet concentration

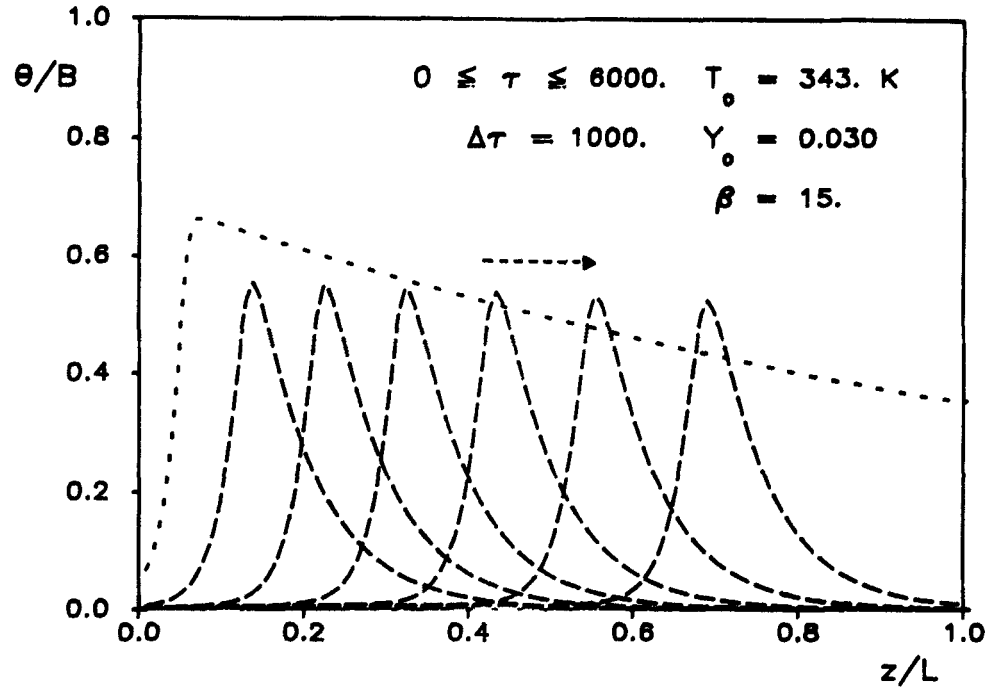

Figure 7. Downstream (extinction) propagating front as a traveling wave.
Change in heat loss parameter

convection-diffusion systems, numerical difficulties arise due to the spatial discretization. A large volume of investigation on the behavior of different methods suitable for solving the classical convection-diffusion transient problem has been done so far. Presently it is understood how to eliminate artificial oscillations caused by temporal integration, and how to supress oscillations due to the approximation of the convective term. Unfortunately, in the latter case the spatial increment required for approximation is usually very small. Many of the numerical schemes proposed degrade the quality of the solution by introducing artificial dispersion in the solution.

In recent years the method of orthogonal collocation (Villadsen and Stewart, 1967) challenged many of the traditional finite-difference schemes. It has been used successfully in cases

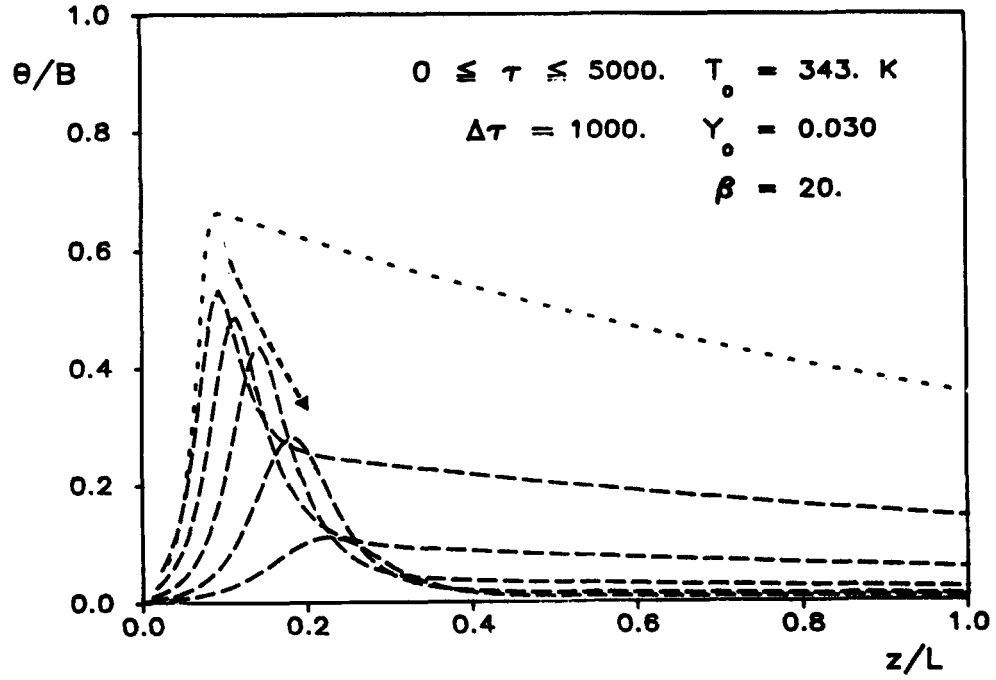

Figure 8. Downstream (extinction) propagating front as a degenerated wave.
Change in heat loss parameter

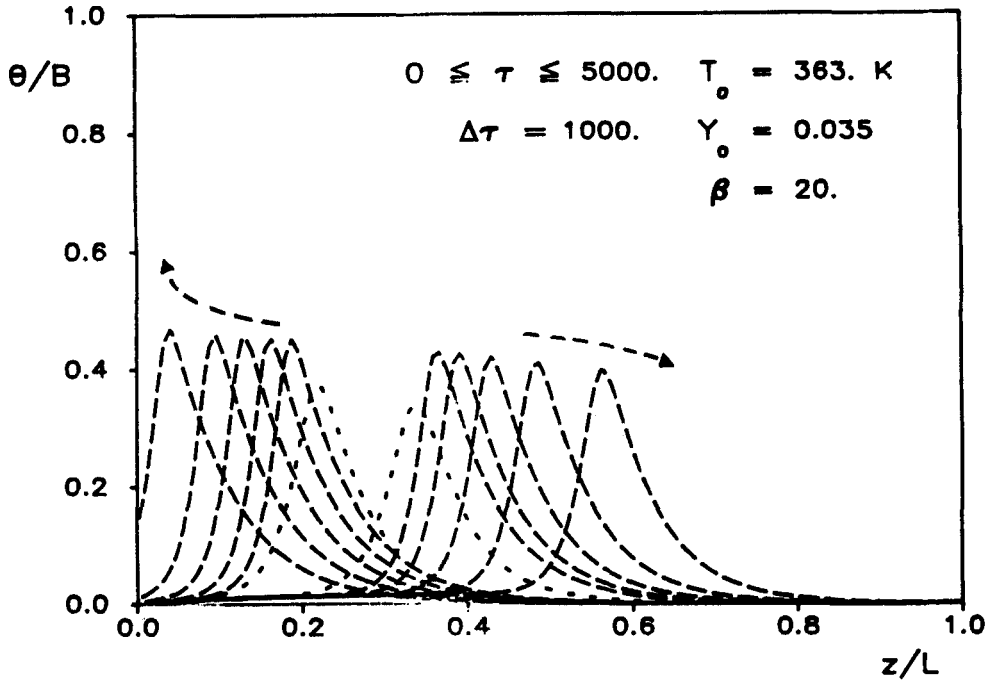

Figure 9. Degenerated waves in the region of multiplicity.
Step perturbation in inlet concentration

of moderate values of the Peclet number (Jutan et al., 1977) and even when the system exhibits high sensitivity to changes of the operating conditions (Gatica et al., 1984). However, this approach is inappropriate at high values of the Peclet and Damkohler numbers when boundary layers related to flow and chemical reaction exist. In order to obtain a good representation of such a boundary layer problem, a large number of collocation points is needed, most of which are wasted outside the boundary layer. Moreover, the null gradient zone downstream of the boundary layer is difficult to represent by orthogonal collocation, and space oscillations on the profiles appear.

For problems of this type finite-difference methods are superior to the orthogonal collocation approach because a large number of grid points can be used and computations can be efficiently performed through tridiagonal matrix calculations.

From Figure 1 it can be inferred that three regions are clearly distinguished inside the reactor. Thus, a piecewise representation of the temperature and conversion profiles might be efficient. This idea, proposed by Carey and Finlayson (1975), has been called orthogonal collocation on finite elements (OCFE), and it is also referred to in the literature as spline collocation (Villadsen and Michelsen, 1978; De Boor and Swartz, 1973). This method could be considered a good combination of a small truncation error approach, typical for orthogonal collocation, and the ability of the finite-difference method to place grid points where needed.

This method provides a useful tool to solve steady state problems, as shown by Carey and Finlayson (1975), who proposed to locate most of the elements in the boundary layer. In a recent paper, Jensen and Ray (1982) used this approach, obtaining the solution outside the reaction zone by analytical solution of the governing equations without the reaction term.

Transient problems featuring boundary layers are characterized by a displacement in time of such a narrow region. An efficient numerical technique requires a regridding of the mesh points in space. The methods that deal with this problem are frequently referred to as mesh refinement techniques or moving coordinate system methods. The first approach consists basically in redefining the grid at each time step in such a way that the reaction zone is well approximated and unnecessary points elsewhere are eliminated (Dwyer et al., 1982; Smooke et al., 1982; Gropp, 1980; McDonald, 1979; Eigenberger and Butt, 1976). The second approach takes advantage of defining a new coordinate system that moves along with the reaction front, so that the front remains fixed in time in the new coordinate system (Warnatz, 1978; Puszynski et al., 1986); however, a moving boundary problem is generated.

In this work spatial discretization of the OCFE type has been applied and temporal integration has been carried out through the method of lines. Two different discretization schemes have been tested:

1. A fixed-element scheme with 20–50 elements equidistantly distributed. The location of the elements remains fixed in time. The number of interior collocation points varied between 3 and 5.

2. An adaptive scheme with 7–9 moving elements. The elements are moving accordingly to the propagation of the reaction front. The reaction front is always approximated by several elements. The number of interior collocation points was the same as in scheme 1.

Both schemes have predicted similar results. The average time of calculation necessary to solve the full governing equations using a CRAY-1 supercomputer (Los Alamos, NM) was 5–15 min of CPU time.

Comparison with analytical results

The comparison of analytically predicted reaction front properties (velocity of propagation and hot spot temperature and

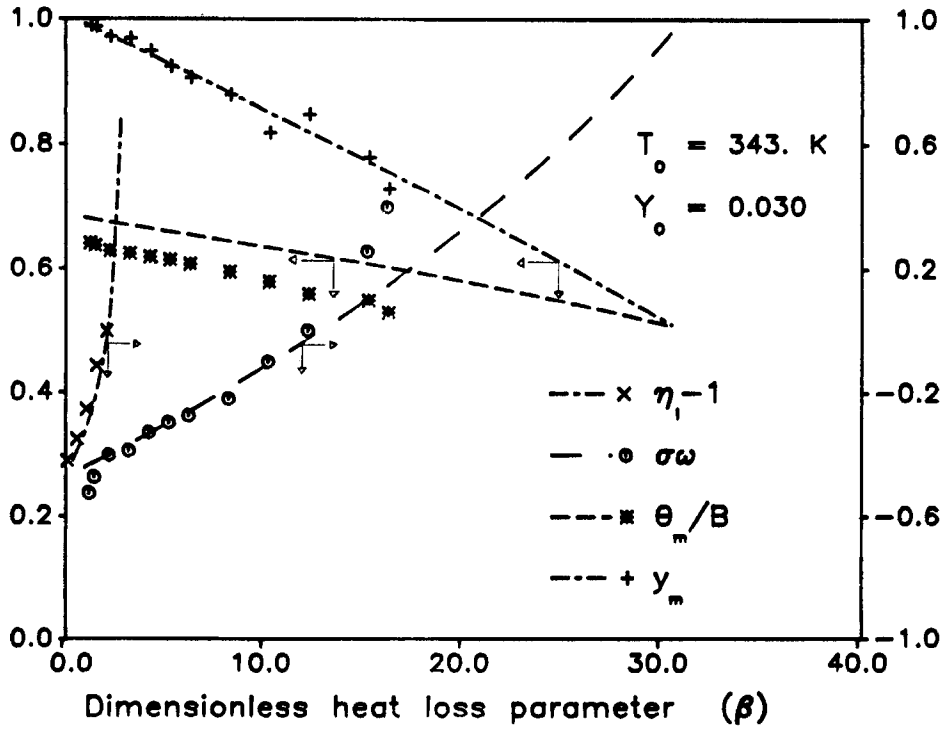

Figure 10. Comparison between numerical and analytical results.

conversion) and ignition length with the exact results obtained by numerical solution of the governing equations, Eqs. 3 and 4 is presented in Figure 10. The inlet conditions correspond to the situation illustrated by Figure 12a [$T_o = 343\ K$, $Y_o = 0.03$, and $(\rho_g u)_o = 9.26\ 10^{-2}\ kg \cdot m^{-2} \cdot s^{-1}$]. It can easily be seen that the analytical approach agrees quantitatively well with the numerical results for a wide range of the values of the heat loss parameter.

The approximate formulas do not predict correctly the critical value of the heat loss parameter for which the possibility of constant pattern profiles disappears. One of the reasons is the assumption of an infinitesimaly narrow reaction zone; numerical results have shown that the larger the heat loss parameter, the wider the reaction zone, Figure 11.

For higher values of activation energy and larger heat capacity of the solid phase, the agreement between analytically pre-

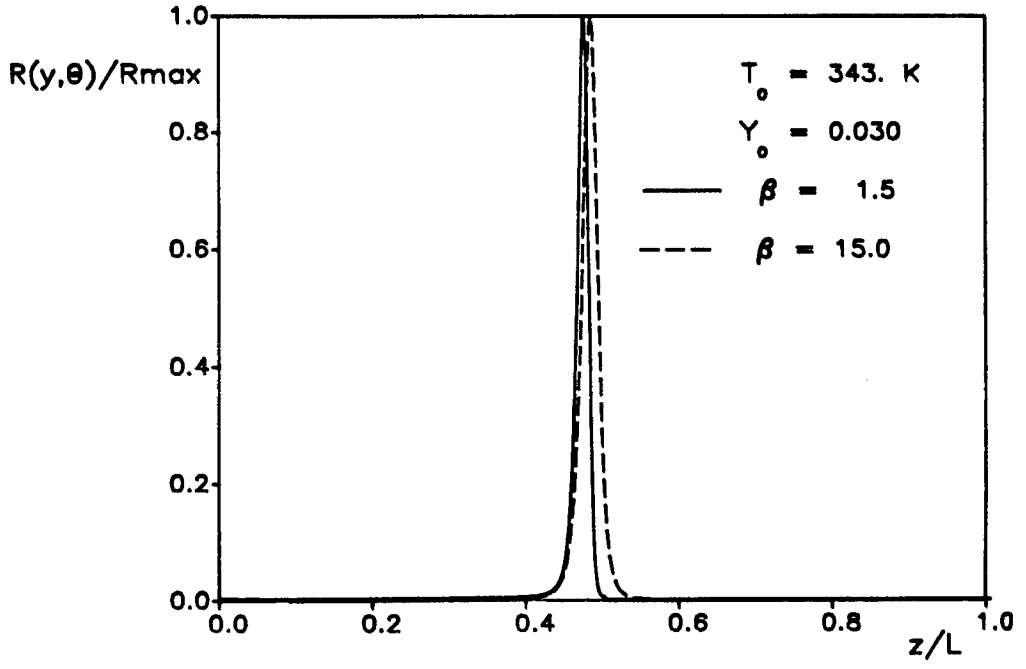

Figure 11. Reaction zone for different values of heat loss parameter.

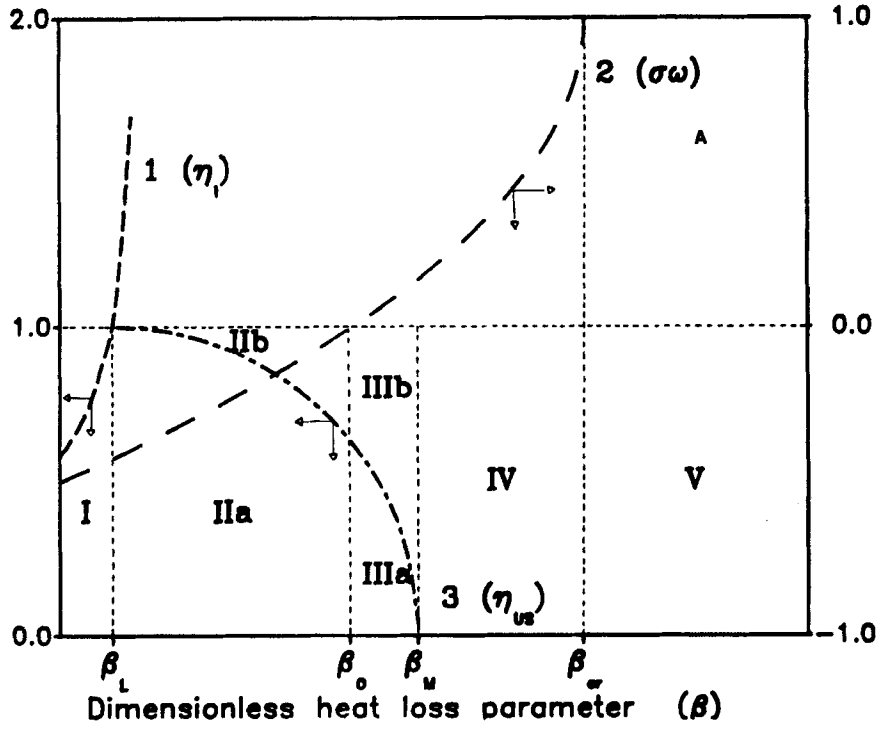

Figure 12a. Transient behavior of reacting flow systems.

dicted and numerically calculated critical values of the heat loss parameter is better.

Acknowledgment

Jorge E. Gatica gratefully acknowledges fellowship support from the Consejo Nacional de Investigaciones Científicas y Técnicas (CONICET) of the Republic of Argentina. The work was supported in part by National Science Foundation grant No. CPE 83-10627 and PRF grant No. 16455 AC5. Time on the CRAY-1 supercomputer was provided by a grant from the Center for Nonlinear Studies, Los Alamos National Laboratory, New Mexico, J. Gubernatis, administrator.

Notation

C = concentration, $kmol \cdot m_g^{-3}$
C_p = specific heat, $kJ \cdot kg^{-1} \cdot K^{-1}$

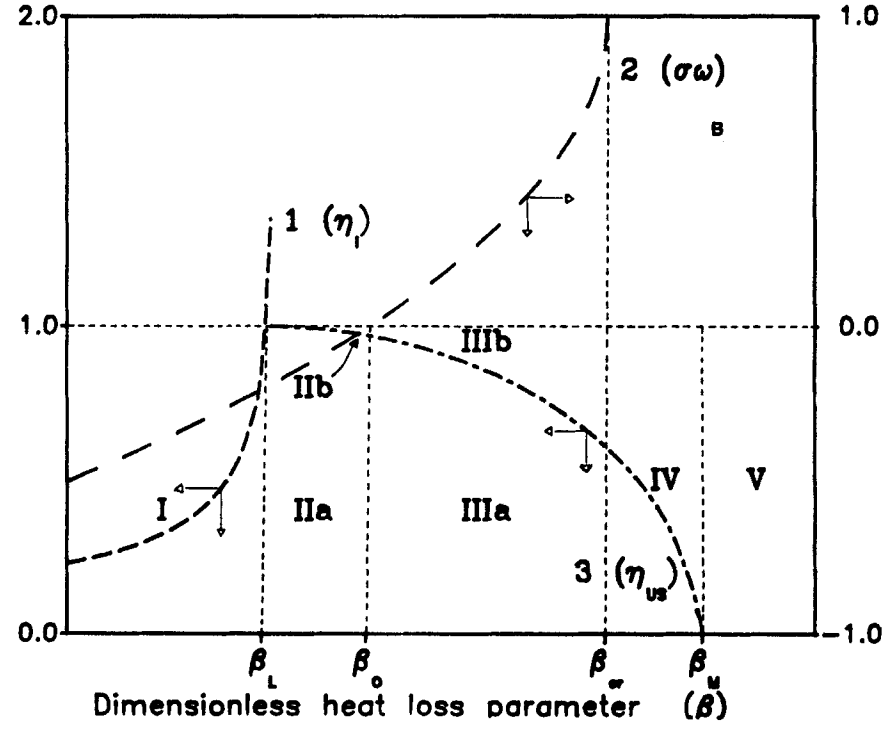

Figure 12b. Transient behavior of reacting flow systems.

D_e = effective mass diffusivity, $mg^3 \cdot m^{-1} \cdot s^{-1}$
D_p = catalyst pellet equivalent diameter, m
D_t = tube diameter, m
E = activation energy, $kJ \cdot kmol^{-1}$
k_e = effective thermal conductivity, $kJ \cdot m^{-1} \cdot s^{-1} \cdot K^{-1}$
K_{eq} = equilibrium constant, $m_g^3 \cdot kmol^{-1}$
k_o = preexponential factor, s^{-1}
L = reactor length, m
n = order of reaction
R = universal gas constant, $kJ \cdot kmol^{-1} \cdot K^{-1}$
t = time, s
T = temperature, K
u = gas superficial velocity, $m \cdot s^{-1}$
U = overall heat transfer coefficient, $kJ \cdot m^{-2} \cdot s^{-1} \cdot K^{-1}$
w = speed of reaction front, $m \cdot s^{-1}$
x = similarity transformation variable, m
y = conversion, $1 - C/C_o$
Y = carbon monoxide molar fraction
z = axial position, m

Dimensionless groups

B = adiabatic temperature rise, $[(T_a - T_o)/T_o]\, E/(RT_o)$
Bo = mass Peclet number (Bodenstein number), $(uL\epsilon)/D_e$
Da = Damkohler number, $[k_o e^{-[E/(RT_o)]}\, LC_o^{n-1}]/u\epsilon$
Pe = thermal Peclet number, $(uL\epsilon\rho_g C_{pg})/k_e$

Greek letters

β = heat loss parameter, $(4UL)/D_t\rho_g C_{pg} u\epsilon$
γ = dimensionless activation energy, $E/(RT_o)$
ΔH_r = heat of reaction, $kJ \cdot kmol^{-1}$
$\Delta\xi$ = reaction zone thickness, m
ϵ = void fraction, $m_g^3 \cdot m^{-3}$
η = dimensionless length, z/L
τ = dimensionless time, $(tu)/L$
θ = dimensionless temperature, $[(T - T_o)/T_o]\, [E/(RT_o)]$
ω = dimensionless reaction front speed, w/u
ρ = density, $kg \cdot m^{-3}$
γ = eigenvalues
σ = heat capacities ratio, $1 + [\rho_s C_{ps}(1 - \epsilon)/(\rho_g C_{pg}\epsilon)]$

Subscripts

a = adiabatic
g = gas
i = at ignition position
m = at hot spot axial position
o = initial
s = solid
z = axial

Appendix: Details of Numerical Solution

The underlying idea is to divide the physical domain in NE elements, each of size h_k, and write the governing equations in every element. Thus, for the kth element, we can define

$$\chi = \frac{\eta - \eta_k}{h_k} \quad \text{with } h_k = \eta_{k+1} - \eta_k$$

and the dimensionless governing equations are

$$\frac{\partial y}{\partial \tau} = -\frac{1}{h_k}\frac{\partial y}{\partial \chi} + \frac{1}{Bo_z}\frac{1}{h_k^2}\frac{\partial^2 y}{\partial \chi^2} + DaR(y, \theta) \qquad \text{(A1)}$$

$$\sigma\frac{\partial \theta}{\partial \tau} = -\frac{1}{h_k}\frac{\partial \theta}{\partial \chi} + \frac{1}{Pe_z}\frac{1}{h_k^2}\frac{\partial^2 \theta}{\partial \chi^2} + BDaR(y, \theta) - \beta\theta \qquad \text{(A2)}$$

Matching between adjacent elements is attained by requiring continuity of profiles and fluxes, that is,

$$\left.\frac{\partial y}{\partial \eta}\right|_{\eta_k^-} = \left.\frac{\partial y}{\partial \eta}\right|_{\eta_k^+} \quad \text{and} \quad y|_{\eta_k^-} = y|_{\eta_k^+} \qquad \text{(A3)}$$

and

$$\left.\frac{\partial \theta}{\partial \eta}\right|_{\eta_k^-} = \left.\frac{\partial \theta}{\partial \eta}\right|_{\eta_k^+} \quad \text{and} \quad \theta|_{\eta_k^-} = \theta|_{\eta_k^+} \qquad \text{(A4)}$$

The dimensionless governing equations, Eqs. 3 and 4, are discretized by means of OCFE, and the following system of $(2\ NE\ NC)$ ordinary differential equations arises

$$\frac{dy_{i,k}}{d\tau} = \frac{1}{Bo_z}\frac{1}{h_k^2}\sum_{j=1}^{NC+2} B_{i,j}y_{j,k} - \frac{1}{h_k}\sum_{j=1}^{NC+2} A_{i,j}y_{j,k} + DaR(y_{i,k}, \theta_{i,k}) \qquad \text{(A5)}$$

$$\sigma\frac{d\theta_{i,k}}{d\tau} = \frac{1}{Pe_z}\frac{1}{h_k^2}\sum_{j=1}^{NC+2} B_{i,j}\theta_{j,k} - \frac{1}{h_k}\sum_{j=1}^{NC+2} A_{i,j}\theta_{j,k} + BDaR(y_{i,k}, \theta_{i,k}) - \beta\theta_{i,k} \qquad \text{(A6)}$$

with $i = 2, \ldots, NC + 1$ and $k = 1, \ldots, NE$, where NC and NE stand for number of interior collocation points and number of elements, respectively.

The system of Eqs. A5 and A6 is integrated through the methods of lines, while the remaining $2(NE + 1)$ unknowns

$$(y_{1,1}, \ldots, y_{1,k}, \ldots, y_{1,NE}, y_{NC+2,NE})$$

and

$$(\theta_{1,1}, \ldots, \theta_{1,k}, \ldots, \theta_{1,NE}, \theta_{NC+2,NE})$$

are determined using matching Eqs. A3 and A4 and the boundary conditions of Eqs. 5 and 6. After discretization, Eqs. 5 and A3 can be rearranged to

$$a_k y_{1,k-1} + b_k y_{1,k} + c_k y_{1,k+1} = d_k \qquad \text{(A7)}$$

where

$$a_k = \begin{cases} 0 & \text{for } k = 1 \\ \left(\dfrac{A_{NC+2,1}}{h_{k-1}}\right) & \text{otherwise} \end{cases}$$

$$b_k = \begin{cases} \left(Bo_z - \dfrac{A_{1,1}}{h_1}\right) & \text{for } k = 1 \\ \dfrac{A_{NC+2,NC+2}}{h_{NE}} & \text{for } k = NE \\ \left(\dfrac{A_{NC+2,NC+2}}{h_{k-1}} - \dfrac{A_{1,1}}{h_k}\right) & \text{otherwise} \end{cases}$$

$$c_k = \begin{cases} 0 & \text{for } k = NE + 1 \\ -\left(\dfrac{A_{1,NC+2}}{h_k}\right) & \text{otherwise} \end{cases}$$

$$d_k = \begin{cases} \dfrac{1}{h_1}\displaystyle\sum_{j=2}^{NC+1} A_{1,j}y_{j,1} & \text{for } k = 1 \\ \dfrac{1}{h_{NE}}\displaystyle\sum_{j=2}^{NC+1} A_{NC+2,j}y_{j,NE} & \text{for } k = NE \\ \dfrac{1}{h_k}\displaystyle\sum_{j=2}^{NC+1} A_{1,j}y_{j,k} & \\ -\dfrac{1}{h_{k-1}}\displaystyle\sum_{j=2}^{NC+1} A_{NC+2,j}y_{j,k-1} & \text{otherwise} \end{cases}$$

In a similar fashion, Eqs. 6 and A4 can be rearranged as

$$a_k\theta_{1,k-1} + b_k\theta_{1,k} + c_k\theta_{1,k+1} = d_k \qquad \text{(A8)}$$

where

$$a_k = \begin{cases} 0 & \text{for } k = 1 \\ \dfrac{A_{NC+2,1}}{h_{k-1}} & \text{otherwise} \end{cases}$$

$$b_k = \begin{cases} \left(Pe_z - \dfrac{A_{1,1}}{h_1}\right) & \text{for } k = 1 \\ \dfrac{A_{NC+2,NC+2}}{h_{NE}} & \text{for } k = NE \\ \left(\dfrac{A_{NC+2,NC+2}}{h_{k-1}} - \dfrac{A_{1,1}}{h_k}\right) & \text{otherwise} \end{cases}$$

$$c_k = \begin{cases} 0 & \text{for } k = NE \\ -\left(\dfrac{A_{1,NC+2}}{h_k}\right) & \text{otherwise} \end{cases}$$

$$d_k = \begin{cases} \dfrac{1}{h_1}\displaystyle\sum_{j=2}^{NC+1} A_{1,j}\theta_{j,1} & \text{for } k = 1 \\ \dfrac{1}{h_{NE}}\displaystyle\sum_{j=2}^{NC+1} A_{NC+2,j}\theta_{j,NE} & \text{for } k = NE \\ \dfrac{1}{h_k}\displaystyle\sum_{j=2}^{NC+1} A_{1,j}\theta_{j,k} & \\ -\dfrac{1}{h_{k-1}}\displaystyle\sum_{j=2}^{NC+1} A_{NC+2,j}\theta_{j,k-1} & \text{otherwise} \end{cases}$$

Equations A7 and A8 are two tridiagonal systems and can be easily solved by means of the Thomas algorithm (Richtmyer and Morton, 1967). For the sake of simplicity, the number of interior collocation points NC has been assumed the same for every element ($NC_k = NC \ \forall \ k$); it can, however, be different. The symbols $A_{i,j}$ and $B_{i,j}$ stand for the orthogonal collocation matrices as defined elsewhere (Villadsen and Michelsen, 1978).

Literature cited

Babkin, V. S., V. I. Drobyshevich, Yu. M. Laevskii, and S. I. Potytnyakov, "Filtration Combustion of Gases," *Comb. Expl. Shock Waves,* **19,** 17 (1983).

Buckmaster, J. D., and G. S. S. Ludford, *Lectures on Mathematical Combustion,* SIAM, Philadelphia (1983).

Carey, C. G., and B. A. Finlayson, "Orthogonal Collocation on Finite Elements," *Chem. Eng. Sci.,* **30,** 587 (1975).

Clavin, P., "Dynamic Behavior of Premixed Flame Fronts in Laminar and Turbulent Flows," *Prog. Energy Comb. Sci.,* **11,** 1 (1985).

De Boor, C., and B. Swartz, "Collocation at Gaussian Points," SIAM *J. Numer. Anal.,* **10,** 582 (1973).

Dwyer, H. A., M. D. Smooke, and R. J. Kee, "Adaptive Gridding for Finite Difference Solution of Heat and Mass Transfer Problems," Sandia Rept. 82-8661 (1982).

Eigenberger, G., and J. B. Butt, "A Modified Crank-Nicolson Technique with Nonequidistant Space Steps," *Chem. Eng. Sci.,* **31,** 681 (1976).

Edwards, M. F., and J. F. Richardson, "Gas Dispersion in Packed Beds," *Chem. Eng. Sci.,* **23,** 109 (1968).

Fieguth, P., and E. Wicke, "Der Ubergang vom Zund/Losch-Verhalten zu stabilen Reaktionzustanden bei einem Adiabatischen Rohrreactor," *Chem. Ing. Tech.,* **43,** 604 (1971), in German.

Frank-Kamenetskii, D. A., *Diffusion and Heat Transfer in Chemical Kinetics,* 2nd ed., Plenum, New York (1969).

Gatica, J. E., J. A. Porras, A. F. Errazu, and J. A. Romagnoli, unpublished results (1984).

Gropp, W. D., "A Test of Moving Mesh Refinement for 2-D Scalar Hyperbolic Problems," SIAM *J. Sci. Stat. Comp.,* **1,** 191 (1980).

Hirschfelder, J. O., C. F. Curtiss, and D. E. Campbell, "The Theory of Flames and Detonation," *4th Int. Symp. Combust.,* Williams and Wilkins, eds., Baltimore, 190 (1953).

Hlavacek, V., and J. Votruba, "Steady State Operation of Fixed-Bed Reactors and Monolithic Structures," *Chemical Reactor Theory: A Review,*" (L. Lapidus and N. R. Amundson, eds., Prentice Hall, Englewood Cliffs, NJ, 314 (1977).

Jensen, K. F., and W. H. Ray, "The Bifurcation Behavior of Tubular Reactors," *Chem. Eng. Sci.,* **37,** 199 (1982).

Jutan, A., J. P. Tremblay, J. F. McGregor, and J. D. Weight, "Multivariable Computer Control of a Butane Hydrogenolisis Reactor. I: State Space Reactor Modeling," *AIChE J.,* **23,** 732 (1977).

Kalthoff, O., and D. Vortmeyer, "Ignition/Extinction Phenomena in a Wall-Cooled Fixed-bed Reactor," *Chem. Eng. Sci.,* **35,** 1637 (1980).

Liu, S. L., and N. R. Amundson, "Stability of Adiabatic Packed-bed Reactors. An Elementary Treatment," *Ind. Eng. Chem. Fundam.,* **1,** 200 (1962).

Margolis, S. D., "An Asymptotic Theory of Condensed Two-Phase Flame Propagation," SIAM *J. Appl. Math.,* **43**(2), 351 (1983).

———, "An Asymptotic Theory of Heterogeneous Condensed Combustion," *Comb. Sci. Tech.,* **43,** 197 (1985).

Margolis, S. D., and R. C. Armstrong, "Two Asymptotic Models for Solid Propellant Combustion," submitted to *Comb. Sci. and Tech.* (1985).

Matkowsky, B. J., and D. O. Olagunju, "Pulsations in a Burner-Stabilized Premixed Plane Frame," SIAM *J. Appl. Math.,* **40**(3) 551 (1981).

Matkowsky, B. J., and G. I. Sivashinsky, "An Asymptotic Derivation of Two Models in Flame Theory Associated with the Constant Density Approximation," SIAM *J. Appl. Math.,* **37**(3), 686 (1979).

McDonald, H., "Combustion Modeling in Two and Three Dimensions. Some Numerical Considerations," *Prog. Energy Comb. Sci.,* **5,** 97 (1979).

Oran, E. S., and J. P. Boris, "Detailed Modeling of Combustion Systems," *Prog. Energy Comb. Sci.* **7,** 1 (1981).

Padberg, G., and E. Wicke, "Stabiles und instabiles Verhalten eines adiabatischen Rohrreactors on Beispiel der katalytischen CO-Oxidation," *Chem. Eng. Sci.,* **22,** 1035 (1967).

Price, H. S., R. S. Varga, and J. E. Warren, "Application of Oscillation Matrices to Diffusion-Convection Equations," *J. Math. Phys.,* **45,** 301, (1966).

Puszynski, J., J. Degreve, and V. Hlavacek, "Modeling of the Exothermic Solid-Solid Noncatalytic Reactions," *Ind. Eng. Chem. Fundam.* (in press) (1987).

Puszynski, J., and V. Hlavacek, "Experimental Study of Traveling Waves in Nonadiabatic Fixed-bed Reactors for the Oxidation of Carbon Monoxide," *Chem. Eng. Sci.*, **35,** 1769 (1980).

Rhee, H. K., and N. R. Amundson, "Equilibrium Theory of Creeping Profiles in Fixed-bed Catalytic Reactors," *Ind. Eng. Chem. Fundam.* **13,** 1 (1974).

Rhee, H. K., D. Foley, and N. R. Amundson, "Creeping Reaction Zone in Catalytic Fixed-bed Reactors," *Chem. Eng. Sci.* **28,** 607 (1973).

Rhee, H. K., R. P. Lewis, and N. R. Amundson, "Creeping Profiles in Catalytic Fixed-bed Reactors. Continuous Models," *Ind. Eng. Chem. Fundam.*, **13,** 317 (1974).

Richtmyer, R. D., and K. W. Morton, *Difference Methods for Initial-Value Problems,* Interscience, New York (1967).

Simon, B., and D. Vortmeyer, "Measured and Calculated Migrating Speeds of Reaction Zones in a Fixed-bed Reactor. A Quantitative Comparison," *Chem. Eng. Sci.*, **33,** 109 (1977).

Sivashinsky, G. I., and B. J. Matkowsky, "On the Stability of Nonadiabatic Flames," SIAM *J. Appl. Math.*, **40**(2), 255 (1981).

Smooke, M. D., J. A. Miller, and R. J. Kee, "On the Use of Adaptive Grids in Numerically Calculating Adiabatic Flame Speeds," *Proc. GAMM Conf. Premixed Laminar Flames,* Aachen, West Germany (1982).

Villadsen, J. V., and M. L. Michelsen, *Solution of Differential Equations by Polynomial Approximation,* Prentice Hall, Englewood Cliffs, NJ (1978).

Villadsen, J. V., and W. E. Stewart, "Solution of Boundary-Value Problems by Orthogonal Collocation," *Chem. Eng. Sci.*, **22,** 1483 (1967).

Vortmeyer, D., and W. Jahnel, "Moving Reactions Zones in Fixed-bed Reactors Under the Influence of Various Parameters," *Chem. Eng. Sci.* **27,** 1485 (1972).

Votruba, J., V. Hlavacek, and M. Marek, "Packed-bed Axial Thermal Conductivity," *Chem. Eng. Sci.*, **27,** 1845 (1972).

Warnatz, J., "Calculation of the Structure of Laminar Flat Flames. I: Flame Velocity of Freely Propagating Ozone Decomposition Flames," *Ber. Bunsenges. Phys. Chem.* **82,** 193 (1978).

Zel'dovich, Ya. B., G. I. Barenblatt, V. B. Librovich, and G. M. Machviladze, *Mathematical Theory of Combustion and Explosion,* Nauka, Moscow (1980), in Russian.

Zel'dovich, Ya. B., and D. A. Frank-Kamenetskii, "Thermal Theory of Flame Propagation," *Zhur. Phys. Chim.*, **12,** 100 (1938), in Russian.

Manuscript received Sept. 5, 1986, and revision received Dec. 24, 1986.